Int. J. Nanosci. Nanotechnol., Vol. 15, No. 1, March. 2019, pp. 45-53

Short Communication

ZnS Nanoparticles Effect on Electrical Properties of Au/PANI-ZnS/Al Heterojunction

Hojjat Amrollahi Bioki[1*] and Mahmood Borhani Zarandi[2]

[1]Photonics Research Group, Engineering Research Center, Yazd University, Yazd, Iran.
[2]Atomic and Molecular Division, Faculty of Physics, Yazd University, Yazd, Iran.

(*) Corresponding author: h.amrollahi@staff.yazd.ac.ir
(Received: 18 December 2016 and Accepted: 22 October 2018)

Abstract

Hybrid polyaniline (PANI) based composites incorporating zinc sulfide (ZnS) nanoparticles (NPs) have been synthesized by using chemical oxidation technique. Schottky junction is constructed by depositing Polyaniline-zinc sulfide nanocomposite (PANI-ZnS NCs) on Au electrode. The results were compared with pure polyaniline. The I–V *characteristics of the PANI-ZnS NCs heterojunction have shown the rectifying behavior. The detailed electrical measurement of the devices is performed under the different ratio of ZnS nanoparticles. An abnormal increase in the barrier height and decrease in the ideality factor with increasing 10 wt.% ZnS nanoparticles have been shown. The ideality factor (η) and barrier height (ϕ_b) of the heterojunction diode at room temperature are found to be 3.41 and 0.82 eV, respectively. These results showed the interaction between ZnS nanoparticles and PANI molecular chains.*

Keywords*: Electrical properties, Nanocomposite, Polyaniline, Schottky diode, Zinc Sulfide.*

1. INTRODUCTION

In recent years, conducting polymers have attracted much attention due to their unique properties, and have been widely used in many fields, such as chemical industry, biomedicine, antistatic materials, electromagnetic shielding materials, artificial muscles, electronic devices based on metal semiconductors (i.e. Schottky diodes), micro-cantilever and biosensors [1-3]. It is found that conductive polymers based on polyaniline (PANI) and polypyrrole (PPy) can chemically reduce metal ions whose reduction potentials are higher than those of conductive polymers [4-8].

In order to achieve the practical application of functional nanoparticles in polymers, the first condition is to prepare high concentration, mono-dispersed particles, and composite with the substrate to achieve its workability. There are many advantages to use functional nanoparticles in polymer: nanoparticles and polymer composite can improve the stability of particles, while nanoparticles size can be controlled in a wide range; nanoparticles and polymer composite can be stable nanoparticles surface modification layer structure, to achieve the micro-control of the special nature of nanoparticles; good process-ability and optical properties, especially those conductive polymers and semiconductor nanocomposites materials have attracted more and more attention, and have become the focus of material research in recent years [9-12].

For most of the polymer–hybrid based devices, stability is higher than that of the fully organic based devices and this is particularly true for hybrids composed of inorganic nanoparticles in a non-conductive polymer matrix [13-15]. This is because the polymer matrix prevents, to some extent, inter-diffusion of the inorganic substituent [16].

PANI nanocomposite with ZnO [10], TiO_2 [17], Fe_3O_4 [18], graphite [19], and

nano-clay [20] (layered silicate) can improve the synergistic effect of PANI and inorganic nanoparticles. Improve the dispersibility of PANI, but also enhance the shielding effect of composite coating, adhesion and performance stability. ZnS is a kind of n-type semiconductor material with good chemical stability. It is easy to disperse and difficult to agglomerate. It has excellent optical, electrical and catalytic properties, and is widely used in gas and ultraviolet luminescence sensing. PANI-ZnS composites have been used in dye-sensitized solar cells [21].

In this paper, we report about details of comparative studies on electrical properties of PANI-ZnS NCs at a different weight of ZnS by chemical oxidization technique. So it is thought worthwhile to study the junction behavior of Au/PANI-ZnS NCs/Al interface through measurement of current–voltage (I–V) characteristics and hence founded some parameters related to junction properties and also to observe their variation with different concentration of ZnS nanoparticles. It was found that the addition of ZnS into PANI, led to significant modification in electrical properties of this nanocomposite hybrid.

2. MATERIALS AND METHODS

2.1 Synthesis of Polyaniline via Chemical Oxidative Polymerization

Chemical synthesis of polyaniline in the form of emeraldine salt was done by the general procedure using redox polymerization of aniline in the presence of an oxidant, ammonium peroxidisulphate (APS) and using HCl as a dopant, was supplied by Scharlau Chemie SA (Barcelona, Spain).

Distilled aniline (4.0 ml) was stirred in 50 ml HCl (1.0 M) at 2-3 °C for 30 min. Another solution of APS (4.2 g APS in 35 ml of 1.0 M HCl) was added drop-wise in the solution of aniline with vigorous stirring on a magnetic stirrer for 1 hour to begin the aniline polymerization and kept at 4-5 °C overnight for polymerization. A dark green colored PANI suspension was obtained with precipitation. The synthesized PANI was obtained as finely dispersed particles, were recovered from the polymerization mixture by centrifugation and washed by 1.0 M HCl and deionized water repeatedly until the washing liquid became completely colorless. Finally, the mixture was filtered using filtered assembly. Then it was refiltered and treated with ammonia solution (NH_4OH) to get undoped polyaniline (emeraldine base form) which was soluble in the organic solvent like Dichlorobenzene and N-Methyl-2-pyrrolidone (NMP). Finally, the polyaniline was washed with methanol to remove the oligomers. The filter cake was dried in an oven at 60 °C for 24 hours to get an emerald-green polyaniline in powder form.

2.2 Synthesis of ZnS NPs

The synthesis of ZnS NPs was carried out by the solvothermal method in which thioacetamide (C_2H_5NS) and zinc acetate ($Zn(CH_3COO)_2$) was dissolved in 40 ml of ethanol, magnetically stirred for 30 min, transferred in a 50 ml autoclave, and hydrothermally treated at 120 °C for 8 hours. After cooling the system to room temperature, the product was separated by centrifugation, washed with absolute ethanol and deionized water for several times, and then dried under vacuum at 70 °C for 10 hours. The nanoparticles were collected by centrifugation at 2000 rpm for 15 min, and further purification was made by the ultrasonic bath. The resultant product was finally dried at 120 °C for 2 hours to get the nanocrystalline ZnS powder.

2.3 Synthesis of PANI-ZnS NCs

The PANI-ZnS NCs were prepared by adding 10%, 20% and 30% of nanocrystalline ZnS nanoparticles in weight percentage into PANI matrix in NMP as a solvent and stirring it for 24 hours to form a homogeneous dispersion.

2.4 Characterization

The current–voltage and the conductivity measurements were performed using Keithley 2400 source-meter instrument and four probe point equipped with interfaced software. Metal contacts were deposited by vacuum evaporation method (VAS BUC-78535). PANI-ZnS dispersions thin films were prepared by spin casting method. The thickness of the film determined by taking SEM of the cross-section of the film was found to be on an average of 1.5 μm. The morphology of nanocomposites were observed using SEM instrument (VEGA3, TESCAN, Czech Republic).

3. RESULTS AND DISCUSSION

Figure 1 shows the SEM images of PANI and PANI-ZnS NCs synthesized at different ratios of ZnS to aniline. The SEM images obviously exhibit the regular distribution of ZnS NPs in PANI matrix. PANI with 10 wt.% of ZnS NPs (Figure 1b) shows the higher degree of uniform distribution and it's much similar to that of neat polyaniline, especially. It indicates that the ZnS NPs had successfully penetrated the surrounding PANI matrix. It was found that the addition of ZnS NPs could effectively reduce the agglomeration of PANI, and make the composite particles dispersed evenly, showing the fiber network crosslinking. The results show that the addition of ZnS NPs is not a simple mixing, but can make the composite more uniform and compact. The presence of white color represented the position of ZnS nanoparticles, especially in 30 wt.% (Figure 1d) shows that there is no agglomeration of ZnS NPs in PANI matrix and there is a uniform distribution of the ZnS NPs in the PANI matrix. The nanoparticles were seen to be dispersed closely to each other in PANI matrix with an increase in ZnS content from 10 to 30 wt.% . This is because with increase in nanoparticles loading, the number of particles increases and so the interparticle distance decreases. According to the results, by increasing the ZnS content of PANI-ZnS NCs up to 50 wt.%, the grain size of prepared nanocomposites increased. As can be seen, ZnS NPs were extremely increased due to the large amounts of agglomeration were occurred (Figure 1e-f). At this nanocomposite, like PANI-ZnS (40 wt.%), ZnS agglomeration was observed for PANI-ZnS (50 wt.%).

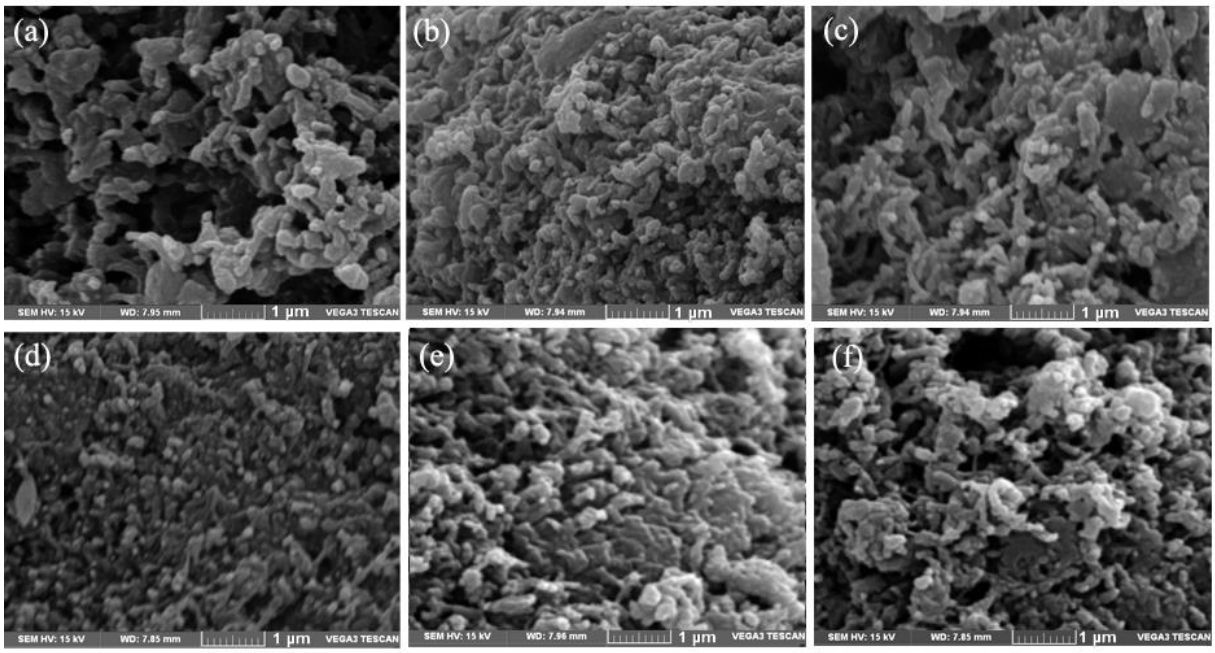

***Figure 1**. SEM micrographs of (a) PANI, (b) PANI-ZnS(10 wt.%), (c) PANI-ZnS(20 wt.%) and (d) PANI-ZnS(30 wt.%), (e) PANI-ZnS(40 wt.%),(f) PANI-ZnS(50 wt.%).*

Schottky junctions are constructed by depositing PANI-ZnS NCs thin films between Au and Al electrodes by spin casting method. A schematic diagram of Au/PANI-ZnS NCs/Al heterostructure diode is depicted in the inset of Figure 2. Gold and aluminum are used as positive and negative electrodes, respectively, for the electrical measurement of the PANI-ZnS NCs hybrid. The current–voltage (I–V) characteristics of PANI-ZnS NCs heterostructure was carried out at room temperatures with an applied voltage range from −1.5 V to +1.5 V, as shown in Figure 2. In this work, gold was chosen as the ohmic contact of the diodes because of its relatively high work function (Φ=5.1 eV) and aluminum was chosen as the Schottky contact because of its relatively low work function (Φ=3.9 eV) in comparison with p-type polyaniline (Φ=4.1–4.45 eV) [22-24]. The I–V characteristic of Au/PANI-ZnS NCs/Al heterostructure exhibits a rectifying and nonlinear behavior. It is clear that the organic-inorganic PANI-ZnS NCs hybrid film charge transport mechanism is predominantly a Schottky emission type conduction mechanism with the formation of an emission barrier layer between the PANI-ZnS NCs hybrid film and the gold electrode

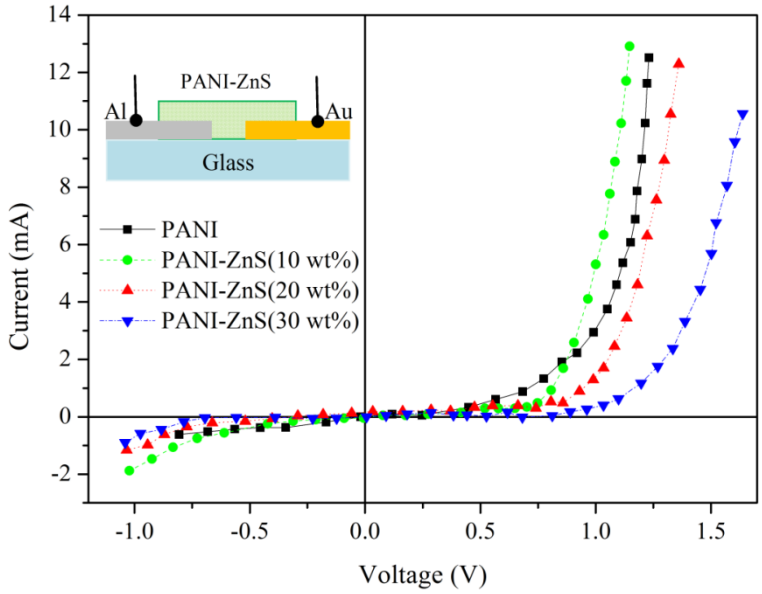

Figure 2. *I–V characteristics of the junction of PANI-ZnS NCs with different ratio of ZnS NPs.*

In order to determine diode parameters, the current as a function of applied bias V is expressed by the following equation, when the forward bias $V > 3\ kT/q$ [23].

$$I = I_s \left[\exp\left(\frac{qV}{\eta kT} \right) - 1 \right] \quad (1)$$

where

$$I_s = AA^* T^2 \exp\left(-\frac{q\phi_b}{k_B T} \right) \quad (2)$$

where A is the contact area, V is the applied voltage, η is the ideality factor, I_s is the saturation current, q is the electron charge, A^* is the effective Richardson's constant, k_B is the Boltzmann constant and ϕ_b is apparent barrier height. The barrier height, ϕ_b is the energy difference between the edge of the conduction band and the redox Fermi level of the organic material and semiconductor layer.

A better model, taking into account the voltage drop across the series resistance (R_s) in the structure, was used. The experimental data are fitted by the modified thermionic emission equation, which is given by [23]:

$$I = I_s\left[\exp\left(\frac{q(V - IR_s)}{\eta kT}\right) - 1\right] \quad (3)$$

The saturation current is obtained from the extrapolated linear intercept with the ln*I* axis at *V=0*. The plot of ln*I* as a function of applied voltage (*V*) for the Au/PANI-ZnS/Al structure for various ratios of ZnS NPs is shown in Figure 3.

The ideality factor (η) was calculated from the slope of the linear region of the forward bias ln*I* versus *V* curve using the following equation:

$$\eta = \frac{q}{kT}\frac{d(V - IR_s)}{d(\ln I)} \quad (4)$$

The ideality factor for an ideal diode is equal to 1.0 and usually, it is greater than the unit. It can be seen from Figure 2 that in the low voltage region is in good agreement with theory predicted by Eq. (1).

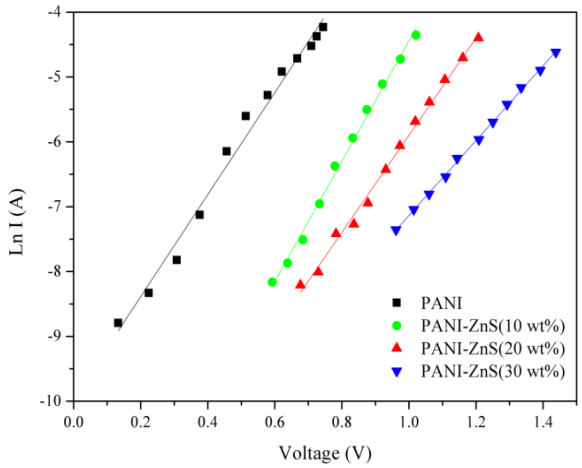

Figure 3. *lnI vs. bias voltage (V) for PANI-ZnS NCs with different ratio of ZnS NPs*

The series resistance is a very important parameter of Schottky barrier devices. The forward bias, *I–V* characteristics due to thermionic emission of a Schottky structure with the series resistance can be written as Cheung's functions [25]:

$$\frac{dV}{d(\ln I)} = IR_s + \eta\left(\frac{kT}{q}\right) \quad (5)$$

$$H(I) = V - \eta\left(\frac{kT}{q}\right)\ln\left(\frac{I}{AA^*T^2}\right) \quad (6)$$

$$H(I) = IR_s + \eta\phi_B \quad (7)$$

The term IR_s is the voltage drop across the series resistance of a Schottky diode. If the series resistance is high, the non-linear forward bias, *I-V* curve will show a wide curvature, and the non-linear region of the forward bias *I-V* curve will be small if the effect of series resistance is less [26-28].

In Figure 4, experimental *H(I)* vs. *I* plot is presented at different ratio of ZnS NPs for the Au/PANI-ZnS NCs/Al structure. The values of R_s and ϕ_b were determined from the slope and intercept of the *H(I)* vs. *I*. The barrier height for Au/PANI-ZnS NCs/Al with various content of ZnS NPs were calculated based on using the η values determined from the data of the forward bias *I-V* characteristics in Eq. (4).

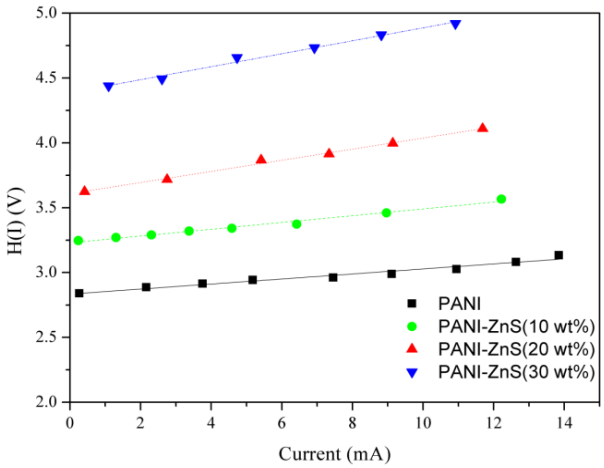

Figure 4. *H(I) vs. I curves of PANI-ZnS NCs with different ratio of ZnS NPs*

The plot of *H*(*I*) vs. *I* will also produce a straight line with *y*-axis intercept equal to $\eta\phi_b$. Moreover, the ratio of forward current (I_f) and reverse current (I_r), called as rectification ratio (*rr*) of the device is estimated at the maximum bias voltage. A small rectification ratio is observed in these Au/PANI-ZnS NCs/Al diodes. This result may be related to the presence of ZnS NPs act as shunt channels.

The electrical parameters of Au/PANI-ZnS NCs/Al heterojunction structure, such as saturation current (I_s), ideality factor (η), potential barrier height (ϕ_b), series resistance (R_s) and rectification ratio (rr)

for the metal/polyaniline and metal/composite polyaniline with various percentage of ZnS NPs are given in Table 1.

The values of the series resistance of Au/PANI-ZnS NCs/Al heterojunctions were calculated from both slope *dV*/*dI* of the least-square fit line to the data points in the linear part of the *I-V* curve in Figure 2 and *H(I)* versus *I* plot in Figure 4 separately. The determined values of R_s and ϕ_b are given in Table 1. As can be seen, the determined values of R_s and ϕ_b obtained from *H(I)* versus *I* and *LnI* versus *V* have been compared and they are in good agreement with each other.

Table 1*. Junction parameters for PANI- ZnS NCs heterostructures with different ratio of ZnS nanoparticles derived from I-V and H-I characteristics.*

Sample	η	I_s (A)	ϕ_b(eV)		R_s (Ω)		rr
			I-V	*H-I*	*I-V*	*H-I*	
PANI	3.83	4.73×10-5	0.73	0.74	18.8	19.3	1.43
PANI-ZnS(10 wt.%)	3.41	1.10×10-6	0.82	0.94	25.1	26.1	2.33
PANI-ZnS(20 wt.%)	4.44	1.55×10-6	0.81	0.81	37.5	42.7	1.94
PANI-ZnS(30 wt.%)	5.76	2.49×10-6	0.79	0.76	54.8	49.9	1.22

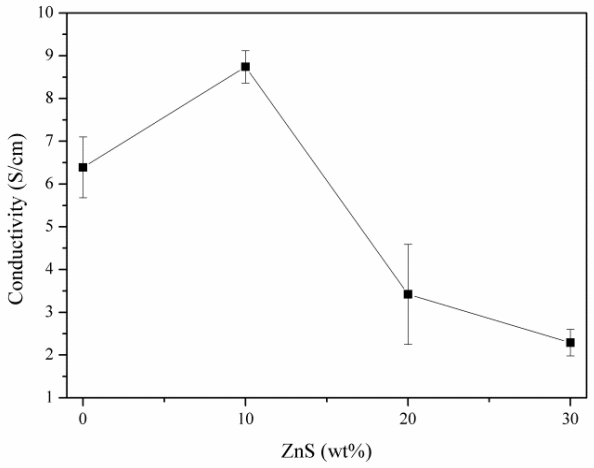

Figure 5*. Conductivity plot of PANI-ZnS NCs with different ratio of ZnS NPs.*

Also, it is found that the DC conductivity of the PANI shows enhanced conductivity for 10 wt.% ZnS NPs as compared to pure PANI and another ratio of ZnS NPs embedded in PANI (Figure 5). The conductivity depends on external factors such as compactness, delocalized length and microparticles orientation. It is clear from the Figure 5, the higher conductivity at (10 wt.%) PANI-ZnS NCs is due to compactness of microparticles on the surface, maximum delocalization length and strong coupling through the grain boundary. The lowered electrical conductivity in (20-30 wt.% ZnS NPs) PANI/ZnS NCs is due to random orientation of microparticle, weak coupling through the grain boundary and formation of agglomerates.

The unexpected increase in the conductivity of PANI for a 10 wt.% of ZnS NPs could have been explained by percolation threshold [29-31]. The low percolation threshold value of conductivity observed for PANI with the inorganic nanoparticles. We may conclude that 10 wt.% of ZnS NPs is good for the formation of large numbers of polarons and bipolarons which due to increasing the conductivity.

It can be found that the barrier height of Au/PANI-ZnS(10 wt.%) NCs/Al is higher than other devices. The higher ϕ_b and lower I_s for this device are expected to arise from the difference in the metal/PANI-ZnS hybrid interfacial characteristics between the other devices.

The variation of η and ϕ_b values determined from the *I-V* curve is presented in Figure6, as function of content of ZnS NPs. The values of η for Au/PANI-ZnS NCs/Al barrier diodes are greater than unity. High values of the ideality factor can be attributed to the presence of the native oxide layer on electrodes, series resistance and also barrier in-homogeneity

[32]. The large values of ϕ_b are associated with small quality factors [33]. On the other hand, the obtained ideality factor for PANI-ZnS (10 wt.%) NCs being smaller than other ones is due to uniformity and homogeneity of the interface structure which is well expected from the SEM micrographs showing in Figure 1.

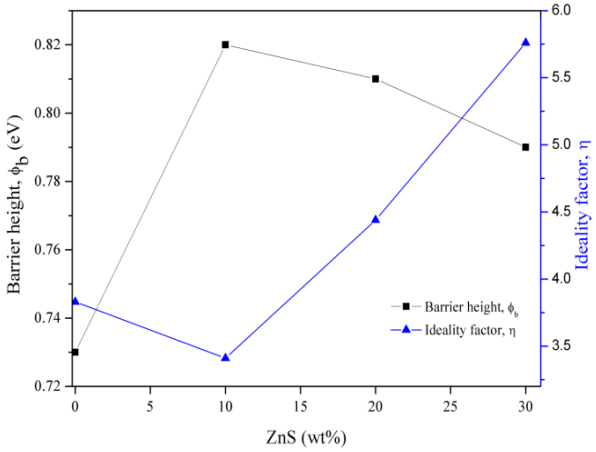

Figure 6*. The barrier height and the ideality factor of PANI-ZnS NCs with different ratio of ZnS NPs*

The comparable values of the rectification ratio confirm that the PANI-ZnS NCs can be used in the fabrication of Schottky diodes due to its properties identical to that of pure polymers. The deviation from an ideal value (n=1.02) may either be due to accelerated recombination of electrons and holes in the depletion region or by the presence of an interfacial layer [34], which introduces the interface states located in it and the semiconductor interface. It is interesting to note that the further increase of ZnS NPs up to 10 wt.% in the composites increases ideality factors and decreases rectification ratios and barrier heights, which may be due to micro-heterogeneity of the films containing an excess of insulating polymers.

4. CONCLUSIONS

PANI-ZnS hybrid nanocomposite was prepared by oxidative polymerization of polyaniline by dispersing ZnS nanoparticles in the solution mixture. The experiments were carried out using different amount of ZnS nanoparticles and maintaining the other reaction conditions unchanged. The SEM study of PANI–ZnS nanocomposites revealed the uniform distribution of ZnS nanoparticles in PANI matrix. Heterojunction diode base on PANI-ZnS nanocomposites was fabricated using aluminum as Schottky contact and gold as ohmic contact. The thermionic emission theory has been satisfactorily applied. The electrical junction parameters such as saturation current, ideality factor, and barrier height for the Au/PANI-ZnS/Al with different content of ZnS nanoparticles have been calculated using the modified Shockley equation taking account of the series resistance. It has been observed that the ZnS nanoparticles with 10 wt.% have better electrical junction diode quality compared to that of the pure polyaniline.

ACKNOWLEDGMENTS

I wish to thank various people for their contribution to this research. Special thanks should be given to Dr. Mahmood Borhani Zarandi, research project supervisor, for his professional guidance and valuable support. I would also like to show our gratitude to Prof. Abbas Behjat, head of the Engineering Research Center at Yazd University, Ms Narjes Kabiri Samani and Ms Shirin Shayegh, for sharing their pearls of wisdom with us during the course of this research.

REFERENCES

1. Xu, H., Ding, L. X., Liang, C. L., Tong, Y. X., Li, G. R., (2013). “High-performance polypyrrole functionalized PtPd electrocatalysts based on PtPd/PPy/PtPd three-layered nanotube arrays for the electrooxidation of small organic molecules”, *NPG Asia Materials*, 5(11): e69.
2. Soleimani, M., Ghorbani, M., Salahi, S., (2016). “Antibacterial activity of polypyrrole-chitosan nanocomposite: mechanism of action”, *International Journal of Nanoscience and Nanotechnology*, 12(3): 191-197.

3. Ghajar, M. H., Mousavi, M., Burzhuev, S., Irannejad, M., Yavuz, M., Abdel-Rahman, E., (2018). "A Short Review on Fabrication Methods of Micro-Cantilever for Ionic Electroactive Polymer Sensors/Actuators", *International Journal of Nanoscience and Nanotechnology,* 14(2): 101-109.
4. Ozaki, M., Peebles, D., Weinberger, B., Chiang, C., Gau, S., Heeger, A., MacDiarmid, A., (1979). "Junction formation with pure and doped polyacetylene", *Applied Physics Letters,* 35(1): 83-85.
5. Chiang, C., Gau, S., Fincher Jr, C., Park, Y., MacDiarmid, A., Heeger, A., (1978). "Polyacetylene,$(CH)_x$: n-type and p-type doping and compensation", *Applied Physics Letters,* 33(1): 18-20.
6. Ding Yu, L., Lei, S., Sheng Dong, Z., Yi, W., Xiao Yan, L., Ru Qi, H., (2007). "Schottky barrier MOSFET structure with silicide source/drain on buried metal", *Chinese Physics,* 16(1): 240.
7. Zhang, J., Wang, S., Xu, M., Wang, Y., Xia, H., Zhang, S., Wu, S., (2009). "Polypyrrole-coated SnO_2 hollow spheres and their application for ammonia sensor", *The Journal of Physical Chemistry C,* 113(5): 1662-1665.
8. Milani Moghaddam, H., (2011). "IV Characteristics of a Molecular Wire of Polyaniline (Emeraldine Base)", *International Journal of Nanoscience and Nanotechnology,* 7(4): 201-204.
9. Zheng, H., Li, Y., Liu, H., Yin, X., Li, Y., (2011). "Construction of heterostructure materials toward functionality", *Chemical Society Reviews,* 40(9): 4506-4524.
10. Layeghi, R., Farbodi, M., Ghalebsaz Jeddi, N., (2016). "Preparation of polyaniline-polystyrene-ZnO nanocomposite and characterization of its anti-corrosive performance", *International Journal of Nanoscience and Nanotechnology,* 12(3): 167-174.
11. Xue, Z., Yang, H., Gao, J., Li, J., Chen, Y., Jia, Z., Li, Y., (2016). "Controlling the Interface Areas of Organic/Inorganic Semiconductor Heterojunction Nanowires for High-Performance Diodes", *ACS applied materials & interfaces,* 8(33): 21563-21569.
12. Sadeghi, B., Sadjadi, M., Pourahmad, A., (2008). "Effects of protective agents (PVA & PVP) on the formation of silver nanoparticles", *International Journal of Nanoscience and Nanotechnology,* 4(1): 3-12.
13. Godovsky, D. Y., (2000). "Device applications of polymer-nanocomposites *Biopolymers· PVA Hydrogels, Anionic Polymerisation Nanocomposites*", (pp. 163-205), Springer.
14. Iqbal, T., Tufail, S., Ghazal, S., (2017). "Synthesis of Silver, Chromium, Manganese, Tin and Iron Nano Particles by Different Techniques", *International Journal of Nanoscience and Nanotechnology,* 13(1): 19-52.
15. Falahatgar, S., E Ghodsi, F., (2016). "Annealing Temperature Effects on the Optical Properties of MnO_2: Cu Nanostructured Thin Films", *International Journal of Nanoscience and Nanotechnology,* 12(1): 7-18.
16. Dey, S., Baglari, S., Sarkar, D., (2016). "Junction characteristics of ITO/PANI-ZnS/Ag and ITO/PANI-CdS/Ag Schottky diodes: a comparative study", *Indian Journal of Physics,* 90(1): 29-34.
17. Zhang, K., Sharma, S., (2016). "Site–selective, Low-loading, Au Nanoparticle-Polyaniline Hybrid Coatings with Enhanced Corrosion Resistance and Conductivity for Fuel Cells", *ACS Sustainable Chemistry & Engineering,* 5(1): 277-286.
18. Hatamzadeh, M., Johari-Ahar, M., Jaymand, M., (2012). "In situ chemical oxidative graft polymerization of aniline from Fe3O4 nanoparticles", *International Journal of Nanoscience and Nanotechnology,* 8(1): 51-60.
19. Akbarinezhad, E., (2014). "Synthesis of conductive polyaniline–graphite nanocomposite in supercritical CO_2 and its application in zinc-rich epoxy primer", *The Journal of Supercritical Fluids,* 94: 8-16.
20. Navarchian, A. H., Joulazadeh, M., Karimi, F., (2014). "Investigation of corrosion protection performance of epoxy coatings modified by polyaniline/clay nanocomposites on steel surfaces", *Progress in Organic Coatings,* 77(2): 347-353.
21. Shit, A., Chatterjee, S., Nandi, A. K., (2014). "Dye-sensitized solar cell from polyaniline–ZnS nanotubes and its characterization through impedance spectroscopy", *Physical Chemistry Chemical Physics,* 16(37): 20079-20088.
22. Bioki, H. A., (2013). "Determination of the conduction mechanism and extraction of diode parameters of Au/PANI-TiO_2/Al Schottky diode", *The European Physical Journal Applied Physics,* 62(02): 20201.
23. Rhoderick, E., Williams, R., Hammond, P., Grimsdale, R., (1988). "*Metal-Semiconductor Contacts, Monographs in Electrical and Electronic Engineering*", Oxford University Press, USA.
24. Subhan, M. A., Chandra Saha, P., Uddin, N., Sarker, P., (2017). "Synthesis, Structure, Spectroscopy and Photocatalytic Studies of Nano Multi-Metal Oxide MgO· Al_2O_3· ZnO and MgO· Al_2O_3· ZnO-Curcumin Composite", *International Journal of Nanoscience and Nanotechnology,* 13(1): 69-82.
25. Cheung, S., Cheung, N., (1986). "Extraction of Schottky diode parameters from forward current-voltage characteristics", *Applied Physics Letters,* 49(2): 85-87.
26. Aydoğan, Ş., Sağlam, M., Türüt, A., (2008). "Some electrical properties of polyaniline/p-Si/Al structure at 300K and 77K temperatures", *Microelectronic Engineering,* 85(2): 278-283.
27. Kaur, J., Singh, S., Kumar, R., Kanjilal, D., Chakarvarti, S., (2011). "Fabrication of Copper and Iron Nano/Micro Structures on Semiconducting Substrate and Their Electrical Characterization", *International Journal of Nanoscience and Nanotechnology,* 7(4): 183-189.

28. Oueriagli, A., Kassi, H., Hotchandani, S., Leblanc, R., (1992). "Analysis of dark current-voltage characteristics of Al/chlorophyll a/Ag sandwich cells", *Journal of applied physics,* 71(11): 5523-5530.
29. Balberg, I., Azulay, D., Toker, D., Millo, O., (2004). "Percolation and tunneling in composite materials", *International Journal of Modern Physics B,* 18(15): 2091-2121.
30. Heo, S., Yun, J., Oh, K., Han, K., (2006). "Influence of particle size and shape on electrical and mechanical properties of graphite reinforced conductive polymer composites for the bipolar plate of PEM fuel cells", *Advanced Composite Materials,* 15(1): 115-126.
31. Wang, C. C., Song, J. F., Bao, H. M., Shen, Q. D., Yang, C. Z., (2008). "Enhancement of electrical properties of ferroelectric polymers by polyaniline nanofibers with controllable conductivities", *Advanced Functional Materials,* 18(8): 1299-1306.
32. Jang, J., Ha, J., Kim, K., (2008). "Organic light-emitting diode with polyaniline-poly (styrene sulfonate) as a hole injection layer", *Thin Solid Films,* 516(10): 3152-3156.
33. Schmitsdorf, R., Kampen, T., Monch, W., (1997). "Explanation of the linear correlation between barrier heights and ideality factors of real metal-semiconductor contacts by laterally nonuniform Schottky barriers", *Journal of Vacuum Science & Technology B,* 15(4): 1221-1226.
34. Campos, M., Bulhoes, L. d. S., Lindino, C. A., (2000). "Gas-sensitive characteristics of metal/semiconductor polymer Schottky device", *Sensors and Actuators A: Physical,* 87(1): 67-71.